# Vacancy-Induced High Activity of $MoS_2$ Monolayer for CO Electroreduction: A Computational Study

Dongxu Jiao,[a] Yu Tian,[c] Yuejie Liu,[b*] Qinghai Cai,[a,b,d] Jingxiang Zhao,[a,*]

[a] College of Chemistry and Chemical Engineering, and Key Laboratory of Photonic and Electronic Bandgap Materials, Ministry of Education, Harbin Normal University, Harbin, 150025, China

[b] Modern Experiment Center, Harbin Normal University, Harbin, 150025, China

[c] Institute for Interdisciplinary Quantum Information Technology, Jilin Engineering Normal University, Changchun 130052, China

[d] Heilongjiang Province Collaborative Innovation Center of Cold Region Ecological Safety, Harbin 150025, China

[*] To whom correspondence should be addressed. Email: zjx1103@hotmail.com (YL) ; xjz_hmily@163.com or zhaojingxiang@hrbnu.edu.cn (JZ) ; Dongxu Jiao and Yu Tian contribute equally tothis work.

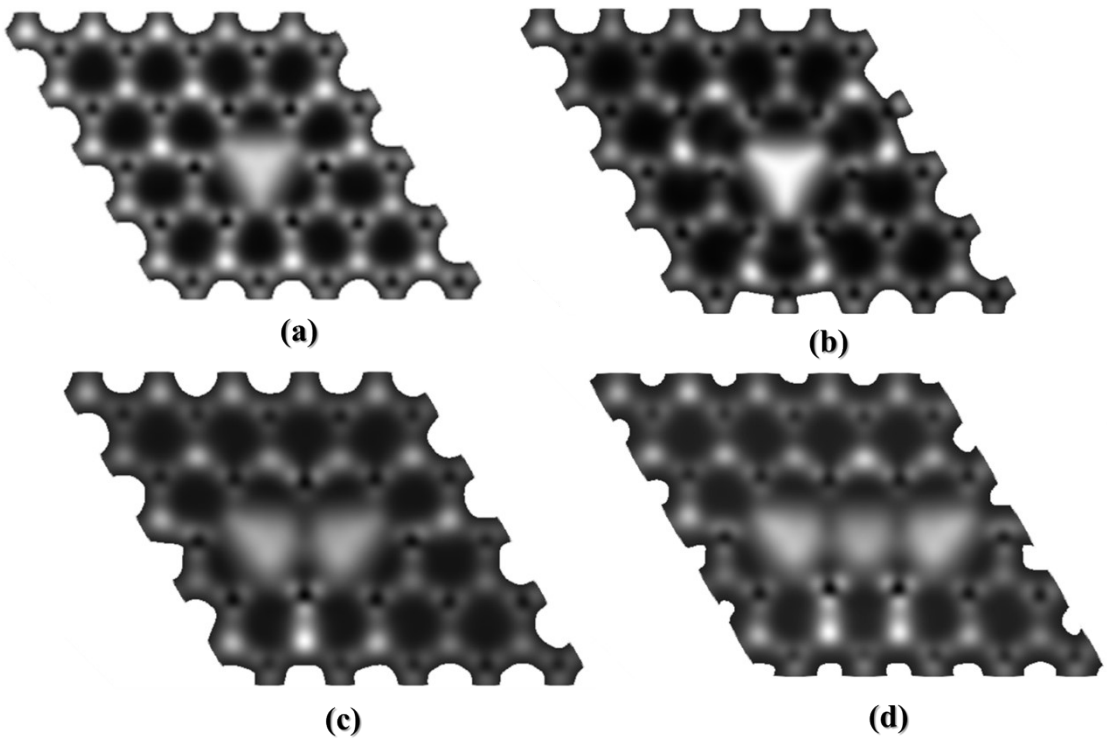


**Fig. S1.** STM image simulation in the constant current mode under a bias voltage of -0.5 V.

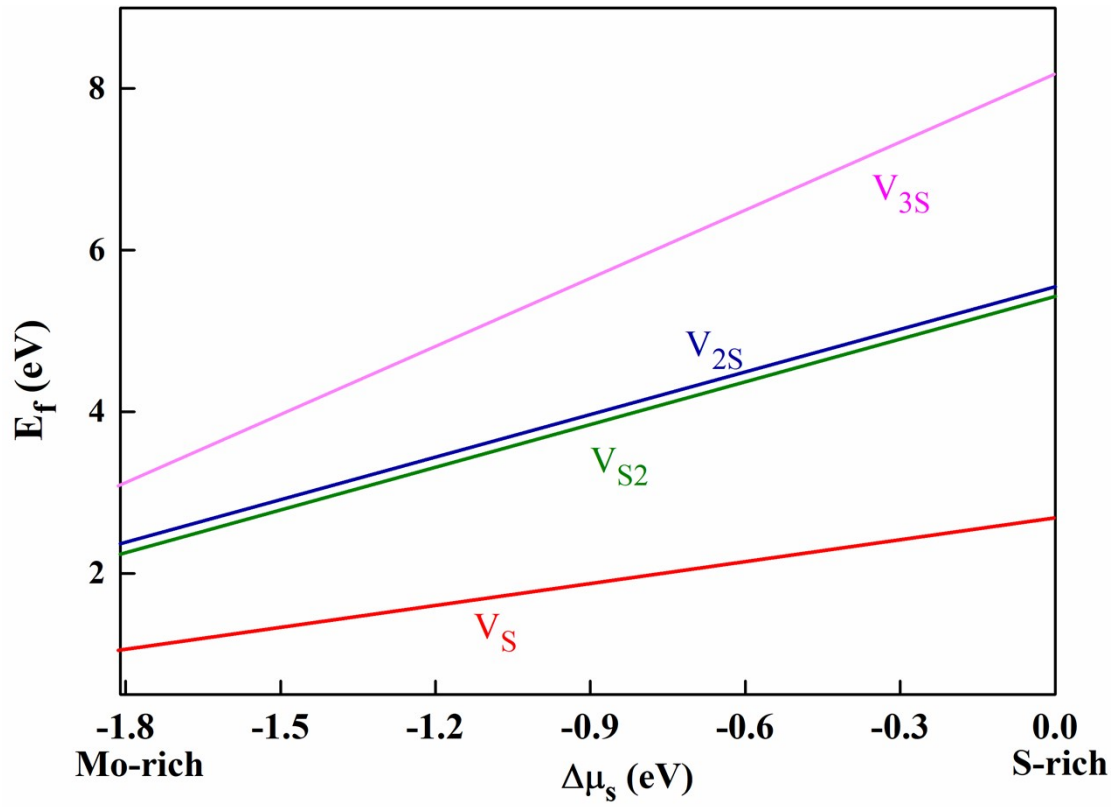


**Fig. S2**. Variation range of the formation energy ($E_f$) of $V_S$, $V_{S2}$, $V_{2S}$ and $V_{3S}$.

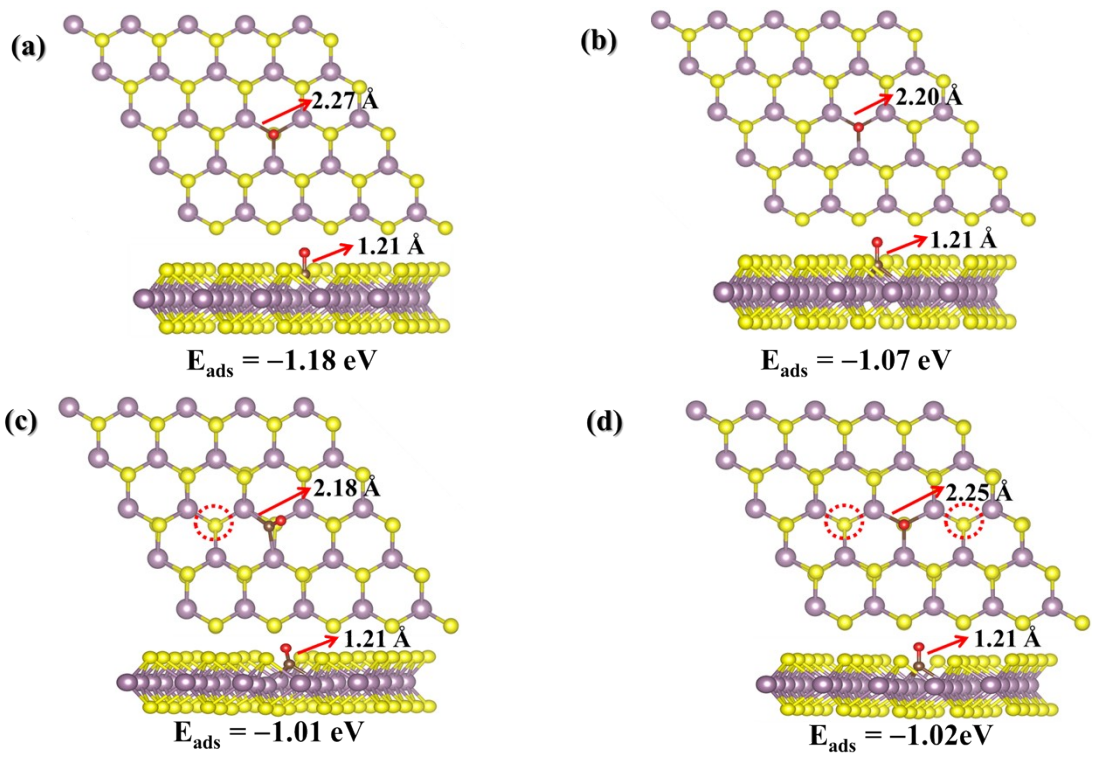


**Fig. S3.** The computed adsorption energies ($E_{ads}$, eV), distances between Mo and C atom ($d_{Mo\text{-}C}$, Å)

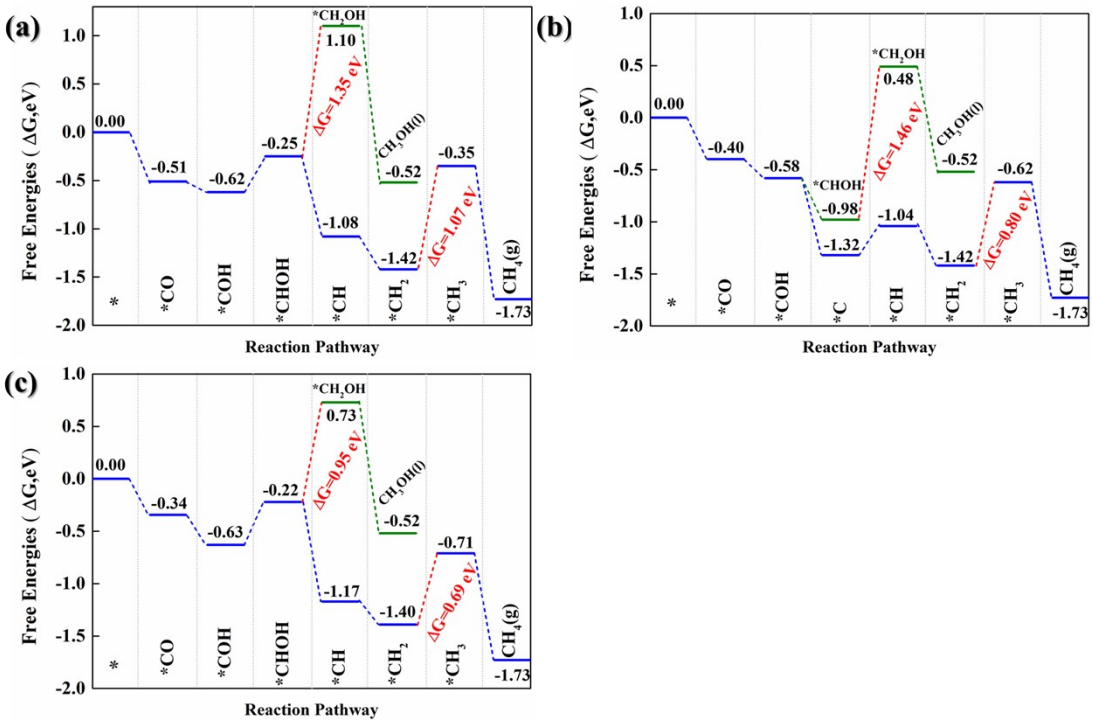


**Fig. S4.** The obtained free energy profiles of COR on (a) $V_S$, (b)$V_{S2}$ and (c)$V_{2S}$.

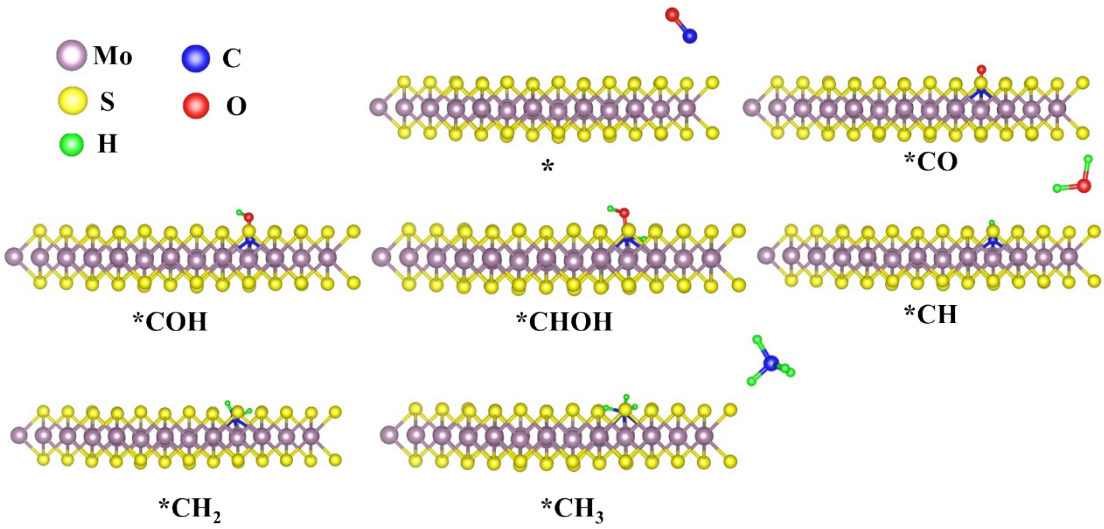


**Fig. S5.** The involed COR intermediates on $V_{3S}$.

**Table S1.** The computed free energy changes of each possible elementary step during the electrochemical reduction of CO to $CH_4$ on the $V_{3S}$ monolayer.

| Elementary step | Free energy change (ΔG) |
|---|---|
| CO (g) → $^*$CO | **–0.35** |
| $^*CO + H^+ + e^- \rightarrow {}^*COH$ | **–0.26** |
| $^*CO + H^+ + e^- \rightarrow {}^*CHO$ | 0.69 |
| $^*COH + H^+ + e^- \rightarrow {}^*CHOH$ | **0.39** |
| $^*COH + H^+ + e^- \rightarrow {}^*C + H_2O$ | 0.51 |
| $^*CHOH + H^+ + e^- \rightarrow {}^*CH + H_2O$ | **–0.91** |
| $^*CHOH + H^+ + e^- \rightarrow {}^*CH_2OH$ | 1.01 |
| $^*CH_2OH + H^+ + e^- \rightarrow {}^*CH_2 + H_2O$ | **–0.20** |
| $^*CH_2OH + H^+ + e^- \rightarrow CH_3OH^*$ | –1.31 |
| $^*CH_2 + H^+ + e^- \rightarrow {}^*CH_3$ | **0.63** |
| $^*CH_3 + H^+ + e^- \rightarrow CH_4$ (g) | **–1.03** |

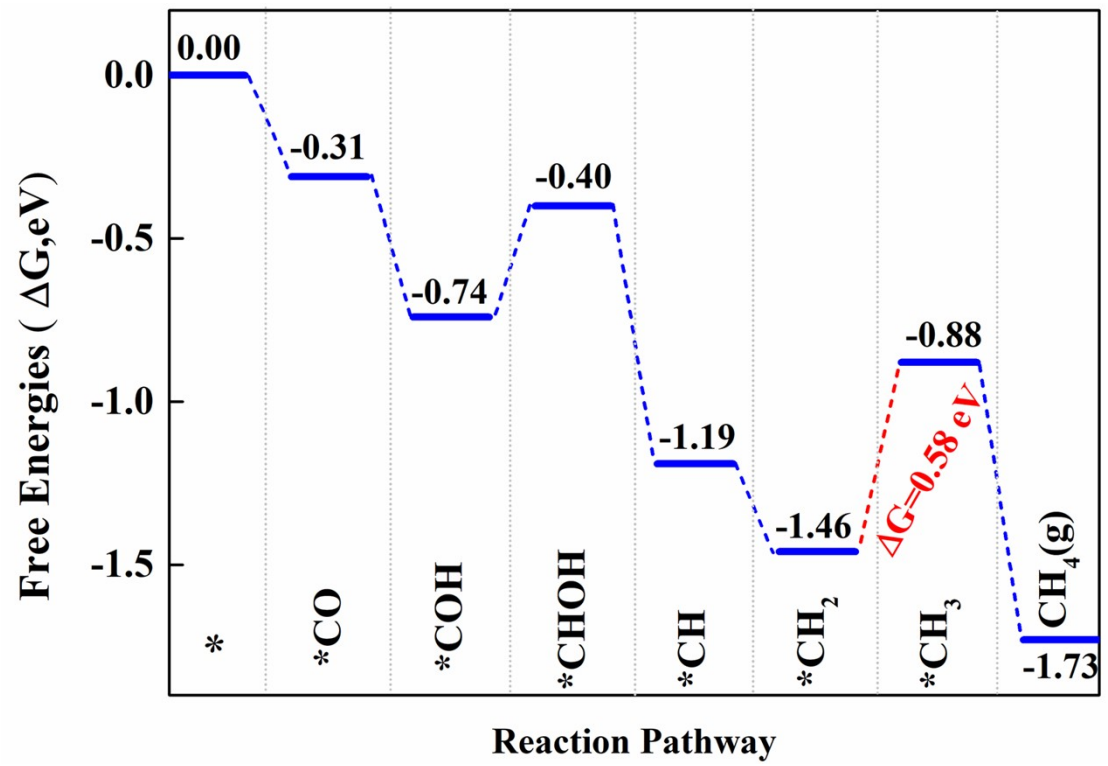


**Fig. S6.** Gibbs free energy (ΔG) diagram for COR on $V_{3S}$ with solvent effect.

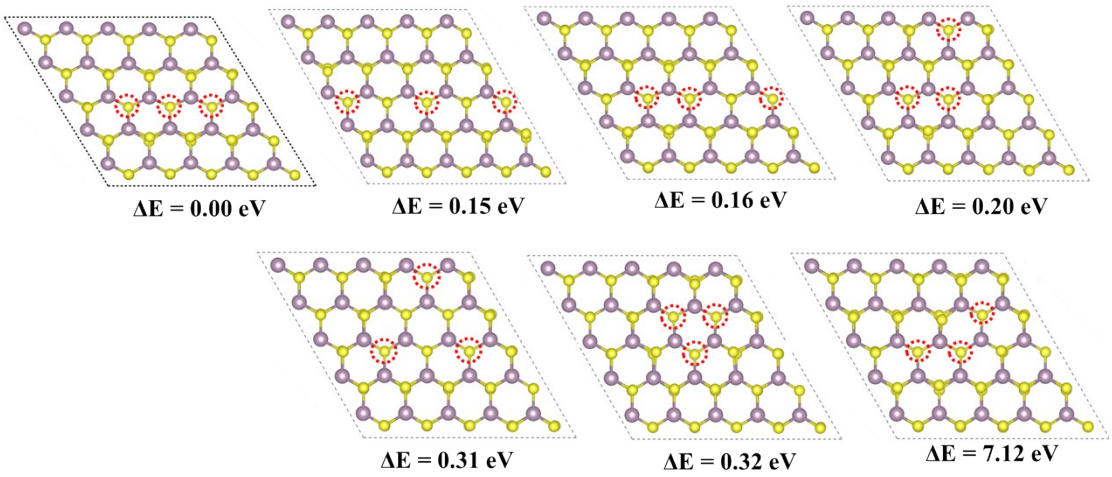


**Fig. S7.** The considered structures of defective $MoS_2$ monolayers with different three S vacancies and the relative energy differences (ΔE), in which the line defect $V_{3S}$ was employed as a reference, and the dotted lines represent S vacancy.

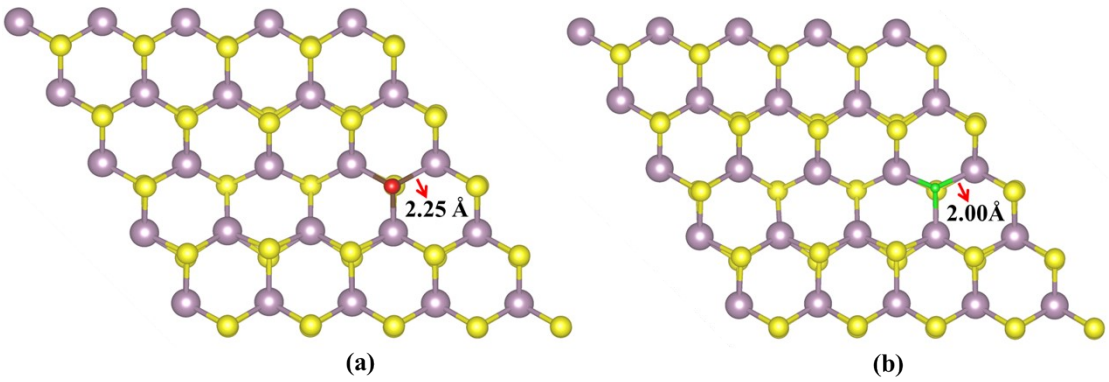


**Fig. S8.** The optimized adsorption configuration of (a) CO molecule and (b) $H^*$ species on $V_{3S}$ monolayer.

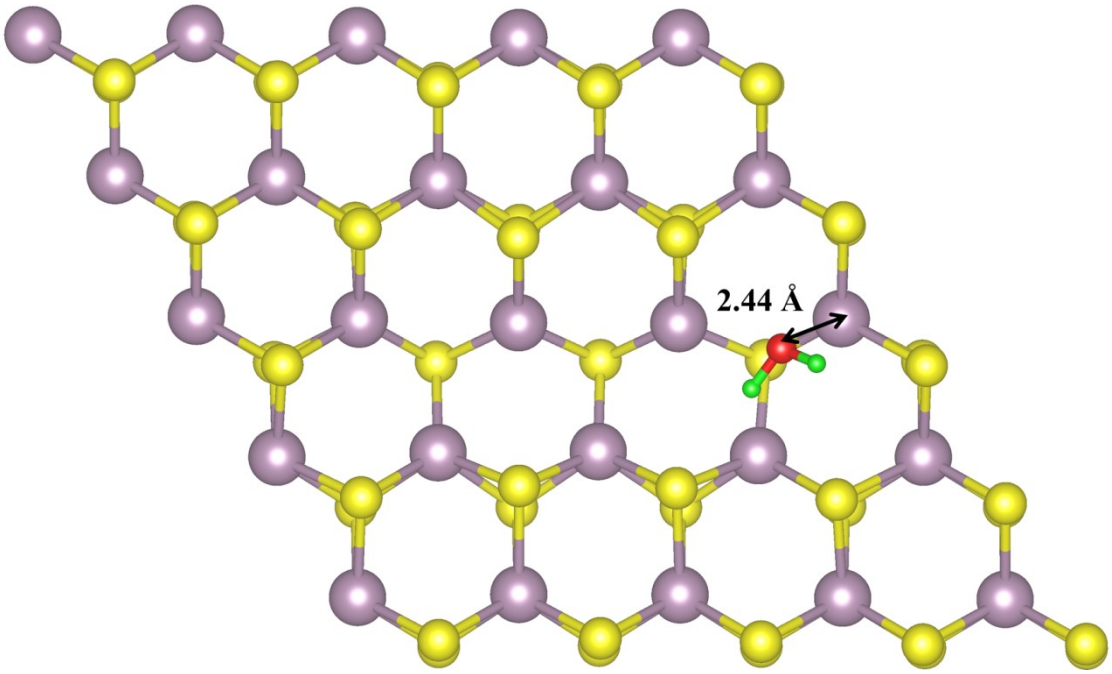


**Fig. S9.** The optimized adsorption configuration of $H_2O$ molecule on $V_{3S}$ monolayer.

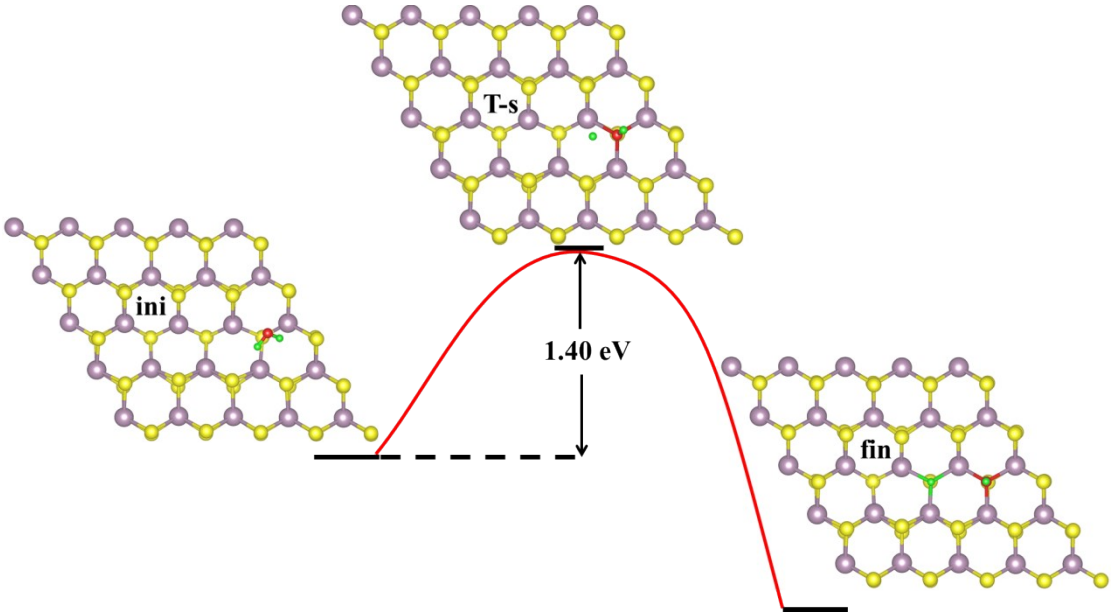


**Fig. S10.** The computed transition state (T-s) for $H_2O$ dissociation on hollow unsaturated Mo sites of the $V_{3S}$ surface.

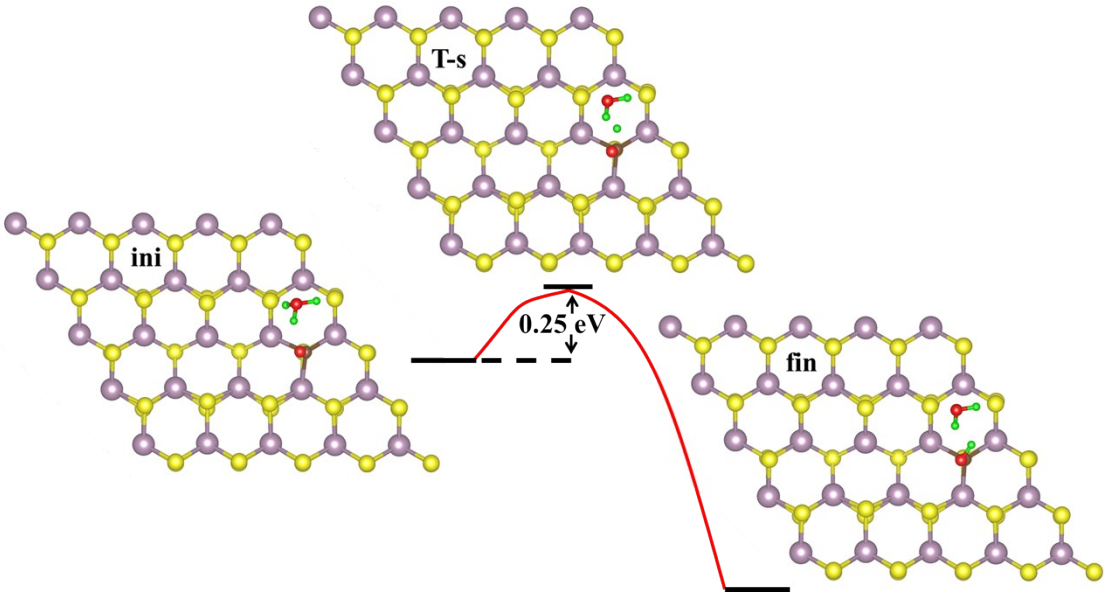


**Fig. S11.** The computed transition state (T-s) for CO hydroenation to $COH^*$ via the Heyrovsky-type mechanism on the $V_{3S}$ surface.